Journal of Environment & Biotechnology Research
VINANIE PUBLISHERS
www.vinanie.com/jebr

Singlet oxygen generation by biopolymer functionalized gold nanoparticle under ultraviolet and visible photo irradiation

G .Vanitha Kumari,[1] S. Asha,[1] N. Nimrodh Ananth,[2] T. Mathavan,[3] M.A. Jothi Rajan[1*]

[1] PG and Research Department of physics, Arul Anandar College, Madurai, India.
[2] MOE Key Lab for Macromolecular synthesis and Functionalization, Department of polymer Science and Engineering, Zhejiang University, P.R. China.
[3] NMSSVN College, Nagamalai, Madurai, India.

ORIGINAL RESEARCH ARTICLE

ABSTRACT

Singlet oxygen plays an important role in photodynamic therapy of cancers, photodynamic abortion of microorganisms and photo oxidation. Herein we exhibit a common platform to improve singlet oxygen production via resonance coupling between surface plasmon and photosensitizers. Pectin functionalized gold nanoparticle (AuNPs) were synthesized. The crystalline size of nanoparticles was investigated using powder X-ray diffraction (XRD) method. The presence of pectin on the surface of gold nanoparticle as visualized from UV-Vis spectra provided the stability and capping density of polymer on surface of AuNPs. The Fourier transform infrared (FTIR) spectroscopy of the sample has confirmed the presence of pectin on the surface of AuNPs. The nanoparticle size was measured utilizing XRD, Dynamic light scattering (DLS). Singlet oxygen generation was observed by photo luminescence spectrophotometer (PL). By adsorbing photosensitizers into pectin containing gold nanoparticles, strong resonance coupling between the photosensitizers and the gold nanoparticle enhance the singlet oxygen generation under UV irradiation. This work establishes a general platform to improve singlet oxygen production and to develop a more effective and efficient hybrid metal-photosensitizer for photodynamic inactivation of cancer cells.

KEYWORDS
gold nanoparticles; pectin; photodynamic therapy; photosensitizer; singlet oxygen; surface plasmon resonance

1. INTRODUCTION

In the recent years, an increasing number of researchers considered the possibility of using nanoparticles in photodynamic therapy (DeRosa and Crutchley, 2002; Bajpai and Shrivastava, 2007). Photodynamic therapy (PDT) is a combination of photosensitizer where molecules can be preferentially localized in tumor tissues based on the systemic administration (Zeitouni et al., 2003). In PDT, singlet oxygen is the main cytotoxic substance which can be generated upon light irradiation. It offers an effective and selective method for destroying diseased tissues without affecting the surrounding healthy tissues (Ouajai and Shanks, 2005). Singlet oxygen is the excited state of the di-oxygen molecule, which is able to damage nucleic acids, proteins and lipids in the cellular environment (Chambina et al., 2006). Singlet oxygen is a cytotoxic agent responsible for photo biological activity (Michael et al., 2006). In the case of nanoparticles with dimensions much smaller than the wavelength of the light, an incident electromagnetic field at a given frequency induces resonant, coherent oscillations of the free electrons in the metal (Wang et al., 2011). The amplitude of the oscillation reaches maximum at a specific frequency, called surface plasmon resonance (SPR), which appears as a result of strong absorption band in the UV-visible spectrum (Jiang et al., 2007).

Gold nanoparticles are increasingly receiving

Corresponding authors: **M.A. Jothi Rajan**
Tel: +91-9486781206
E. mail: angellojothi@gmail.com

Received: 17-11-2016
Revised: 25-11-2016
Accepted: 15-12-2016
Available online: 01-01-2017

attention due to its optical, electrical, catalytic properties, which are the important starting points for efficient contrast agent for biological imaging, drug delivery and spectroscopic applications as well as for photo biological applications (Park et al., 2013a). Consequently, the approach of conjugating photosensitizer molecules to noble metal nanoparticles may be of great significance for singlet oxygen based clinical therapy, such as PDT Polymer functionalized gold nanoparticles have been explored for nano biomedicine (Oh et al. 2013). Their covered shell structures might protect nanoparticles from enzymatic and degradation in water medium. Metal-enhanced singlet oxygen generation (MESOG) was attributed to the enhanced excitation rate due to the metal and the subsequent enhanced intersystem crossing and enhanced excited state triplet yield (Zhang et al., 2007). Actually, there are two proposed mechanisms for the enhancement of the quantum yield of singlet oxygen production: (1) increase of the overall absorption efficiency (cross-section) of the photosensitizer by the nanoparticles or (2) energy transfer from the nanoparticle to the photosensitizer molecules (Huang et al. 2011). Gold nanoparticles were used as a representative of plasmonic nano structure among their photo absorption in visible and UV region (Schmidbaur et al., 2013). Biodegradable polymers have received much attention due to their stabilizing properties (Zhao et al., 2013). Curcumin is selected as a photosensitizer, which has also been used as an anti-oxidant (Chignell et al., 1944; Iijima et al., 2000). Metal enhanced singlet oxygen generation by silver/ pectin was demonstrated (Manju and Sreenivasan, 2012). Plasmon enhanced singlet oxygen generation and parameters for optimizing singlet oxygen are based on the distance dependence of a sensitizer to metallic nanoparticles (Hu et al., 2016). Herein, we report a general singlet oxygen production platform based on the surface plasmon-photosensitizer resonance coupling between AuNPs and photo sensitizers. Strong surface plasmon-photosensitizer resonance coupling significantly increases the singlet oxygen production by UV irradiation. Metal enhanced singlet oxygen generation in curcumin water solution with gold-pectin nanoparticles was observed and quantified using PL.

2. MATERIALS AND METHODS

For the synthesis, the following materials were used: pectin (Alfa Aesar, M.W 60,000 -1,30,000 kDa), Hydrochloroauric acid ($HAuCl_4$) (97.0%), $NaBH_4$ (Loba chemie 97%). Singlet oxygen sensor green-molecular probe (Life technology), curcumin (HIMEDIA P97%) and double distilled deionized water were used for all preparations. All glass wares were cleaned by aquaregia before experiments.

2.1. Synthesis of pectinalized gold nanoparticle using sodium borohydride (NaBH4)

The pectin entrapped gold nanoparticle was prepared via simultaneous synthesis and stabilization of gold nanoparticle using pectin. Pectin/Au nanoparticle was synthesized by the following method: 5 mL of 0.1 mM hydrochloroauric acid ($HAuCl_4$) (97.0%) was added to aqueous solution 5 mL of (0.01, 0.20) wt% pectin (Alfa Aesar, M.W 60,000-1,30,000 kDa) with gentle stirring for 10 min at room temperature (30 ^oC). To this homogenized solution 10 mL of aqueous 1.2 mM cold $NaBH_4$ (Loba chemie 97%) was added at once and stirred for 5 h. The formation of the pectin-AuNPs was observed as an instantaneous color change of the solution from pale yellow to bright violet after addition of reducing agent, which confirmed the formation of nanoparticle.

2.2. Singlet oxygen generation

About 3.3 mL ethanol was added to the 1 vial of GR for making diluted solution. 50 μM of 0.002 g curcumin was mixed with 100 mL of ethanol. Pectin/Au NP (0.01, 0.20 wt% of pectin) colloidal sample (100 μL) was taken in an Eppendorf tube and it was dried at 40 ^oC for making a film. Eppendorf surface was fully shielded by black coating by focusing UV irradiation. Curcumin (0.5 mL) was added to the sample and 100 μL of GR was added to the curcumin mixed sample. Of these, 0.2 mL of solution was not irradiated and 0.2 mL of solution was irradiated by UV light for 5 min. Excitation wavelength is 504 nm with emission at 535 nm.

2.3. Methods

UV-Visible spectra were recorded using a Shimadzu, UV2600 model in the range of 400-700 nm at1 nm resolution. The x-ray diffraction (XRD) patterns for dried pectin/AuNPs were obtained using a powder x-ray diffractometer, Bruker D8 advanced XR-D Germany in the range 10^o to 60^o with 0.02^o step size and 0.8 sec step time with a 1-D position sensitive detector (Lynx Eye) based on silicon drift detector technique, which reduces the measurement time significantly without a reduction in the diffracted intensity. The particle size

and zeta potential measurements were carried out using Malvern-6.32 Model Zeta potential and particle size analyzer. DLS and zeta potential were obtained using nano zetasizer. For finding hydrodynamic diameter size and size distribution of the particle, 0.5 mL of each sample in 3.5 mL of water was measured at room temperature. Infrared spectra were obtained using FT-IR Shimadzu IR-400. The dried samples were then mixed with KBr to produce fine powder, which was pressed in to discs. All spectra were recorded using Shimadzu Model with a wave number range of 400 - 4000 cm^{-1} with 1 cm^{-1} resolution. The singlet oxygen detection studies were carried out using Shimadzu RF-5301 PC Model spectrofluorometer with a range of 515 nm to 815 nm and 504 nm as excitation wavelength and the samples pre-irradiated using 12 Watt UV Lamp for the time period of 5 min.

3. RESULTS AND DISCUSSION

Our approach was to release singlet oxygen under UV and visible light irradiation was illustrated using curcumin as the singlet oxygen source. This ligand adsorbed to the pectin functionalized gold nanoparticle surface through hydroxyl group. Exposing the decorated nanoparticles to visible and UV light induces the singlet oxygen generation. It is well known that chemical reagent ($NaBH_4$) can be used to reduce the gold anions to AuNPs in the presence of pectin as a stabilizing agent. Pectin as a (biocompatible, biodegradable, and non-toxic effective shaping agent) material has been utilized to inhibit the agglomeration of the AuNPs in the solution. The formation of pectin-functionalized AuNPs has been visually observed from the UV-Vis results in Figure 1. The curves (Figure 1) indicate the characteristic surface plasmon resonance (SPR) of the bare AuNPs. Nanoparticle shows plasmon peak between 500-650 nm. It is well known that the UV-Vis spectrum of metal nanoparticles owing to the SPR, leads to the distinguished red or blue shift depending on the dielectric properties of the surrounding host matrix, the environmental atmosphere and the particle size and shape of the nanoparticles. The intensity of the pectin functionalized AuNPs peak at 530 nm has reduced compared with the bare AuNPs as shown in Figure 1. The difference in peak intensity was due to the concentration of polymer surrounding the gold nanoparticle, which was been observed through color of colloidal solution. The red shift and decrease in intensity of peak was due to higher amount of binding of pectin on gold surface as shown in Figure 1. SPR peak intensity has affected by the concentration of pectin.

Powder XRD scan on dried functionalized AuNPs powder was obtained in the 2θ range between 10° and 80° with step size 0.02° and counting time per step 10 sec. The corresponding pattern is shown in Figure 2. The peak of Au (311) appeared around 33.8° for pectin/Au powder. The crystalline size of nanoparticles was calculated using the Scherer formula

$$d = 0.94\lambda/\beta \cos \theta_B \qquad (1)$$

where λ is the x-ray beam wavelength (= 1.54 Å for Cu Kα), β is the FWHM of the of the Bragg peak and θ_B is the peak position. The diameter d was calculated to be around 58.3 nm for pectin / Au.

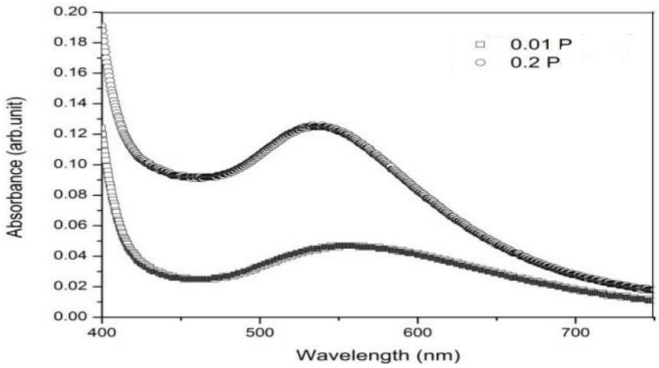

Figure 1. UV-Vis spectrum of P/AuNPs confirmed the presence of gold nanoparticles and capping of pectin.

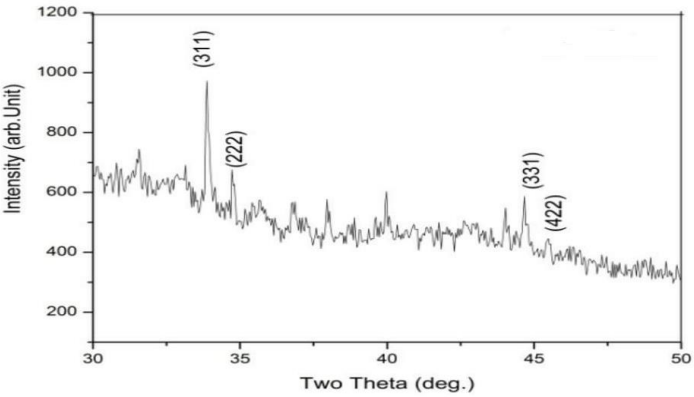

Figure 2. XRD spectrum of P/AuNPs. Powder XRD scan on dried functionalized AuNPs powder was obtained in the 2θ range between 10° and 80° with step size 0.02° and counting time per step 10 s.

Figure 2 depicts X-ray diffraction pattern of pectin/AuNPs. The prominent diffraction peaks at 33.8°, 34.7°, 44.7° amd 50.4° and their corresponding planes were (311), (222), (331) and (422) (JCPDS CD: 021095), respectively, in pectin/AuNPs. Pectin showed peaks equal to 9.0°, 12.7°, 13.6°, 18.4°, 22.6°,

28.2°, 40.1°, which clearly indicate the semi crystalline behavior of pectin (Levy et al., 2004; Cho and Andrews, 2011).

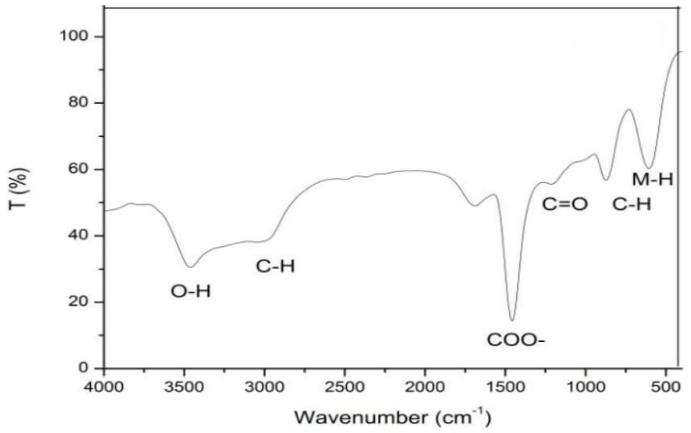

Figure 3. FT-IR spectrum of P/AuNPs confirmed the presence of pectin molecules.

The average hydrodynamic diameter (D_h) of pure pectin and gold nanoparticle were measured using DLS and zeta sizer respectively. After functionalization of gold by pectin an aqueous medium, a drastic change in D_h was observed using DLS. It was observed that D_h increased with increasing concentration of pectin. The zeta potential of the bare gold nanoparticle (~ 17 mV) was very low, indicating that the synthesized gold was unstable and formed clusters of size ~ 234.9 nm. Zeta potential of the pectin-AuNPs increased with the increasing concentration of pectin and its zeta potential values were ~ -12.4, -21.9, indicating that the particle was unstable and formed bigger clusters corresponding hydrodynamic diameter ~ 1937, 2718 nm. Pectin-AuNPs hydrodynamic diameter were ~ 705, 1370 nm. This size agreed with the zetapotential value. From Figure 3, the peak appears at 3466 cm^{-1} can be attributed to O-H participation of the hydroxyl group of the pectin in the chemical reaction (Park et al., 2013b; Andrade et al., 2009; Dai et al., 2013). The peak around 2995 cm^{-1} can be associated with the stretching vibration of (C-H), while the peak around 1215 cm^{-1} was due to stretching vibration of (C=O) and the peaks at 1461 cm^{-1} were assigned to the bending vibration of (C-O). The peak at 1215 cm^{-1} corresponds to COO- stretching (Manson et al 2011; Sutar et al 2008). The appearance of peaks due to the pectin in the functionalized system supports the fact that pectin actually was physically adsorbed on gold nanoparticle.

Metal enhanced singlet oxygen generation was measured on pectin functionalized gold nanoparticles in the presence of curcumin with and without UV irradiation as shown in Figure 4. UV irradiated system has induced the enhanced singlet oxygen generation by the presence of plasmonic gold nanoparticles. Plasmon resonance of gold nanoparticle - photosensitizing properties of curcumin is the reason for the enhancement of singlet oxygen. Resonance coupling can lead to unconventional energy transfer from metal nanoparticles to light absorbing molecules. The results show that presence of gold nanoparticles improves the metal enhanced singlet oxygen generation. Gold nanoparticles localize the irradiation of UV light on specified tissue to avoid the damage of normal tissue. From all the measurements, the synthesized system behaves like targetor, localizer, and efficient singlet oxygen generator. Distance between the metal surface and photosensitizer affecting the singlet oxygen generation.

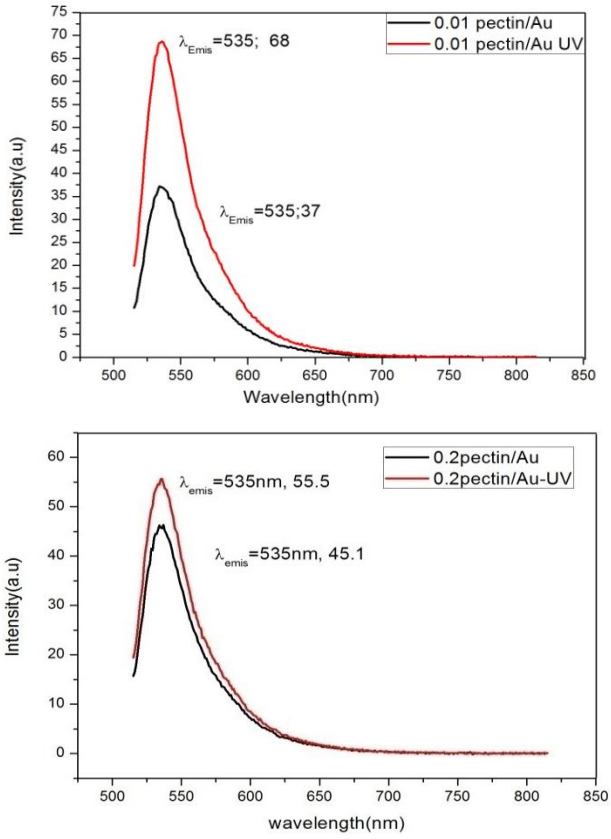

Figure 4. PL spectrum of P/AuNPs indicates the singlet oxygen generation under various concentrations.

From UV-Vis and PL analysis, minimum interaction of pectin allows the free resonance of gold nanoparticles. Gold nanoparticle absorbs visible and UV light at their surface plasmon resonance and convert it into heat localized near the surface of the nanoparticles. This photothermal effect has been used

to destroy cancer cell structure in a localized invasive manner and to release the small molecules from the surface of gold nanoparticles for potential use as drug delivery system.

4. CONCLUSIONS

Enhanced singlet oxygen generation by plasmonic gold nanoparticles was proposed for photodynamic applications. Spherical gold nanoparticle synthesized through the successful functionalization of pectin. Physical absorption of pectin on gold nanoparticle was confirmed by XRD and FTIR and UV-Vis. Zetapotential and hydrodynamic diameter of synthesized nanoparticles were observed from DLA and zetapotential measurements. Generation of singlet oxygen in pectin/AuNPs under presence and absence of UV light irradiation was observed utilizing fluorescence spectrophotometer. The singlet oxygen fluorescent sensor green reagent was used to monitor the singlet oxygen production in the colloid. Singlet oxygen production has found to become more effective for UV-irradiated system. The present report will provide important information for improving the activity of plasmon induced singlet oxygen generation. Synthesized gold nanoparticle will also be used for theranostics application due the diagnosing and treating behavior of gold nanoparticle.

ACKNOWLEDGEMENTS

This work was supported by UGC-RGNF-TAM-3887. We would like to thank UGC-CSR, Indore (India) and Arul Anandar College, Karumathur, Madurai, India.

REFERENCES

Andrade, J.R., Raphael, E. and Pawlika, A. (2009) Plasticized Pectin-based gel electrolytes. Electrochemica Acta, 54, 6479-6483.

Bajpai, A.K. and Shrivastava J. (2007) Studies on a -amylase induced degradation of binary polymeric blends of crosslinked starch and pectin. Journal of Materials Science: Materials in Medicine, 18, 765-77.

Chambina, O., Dupuis, G., Champion, D., Voilley, A. and Pourcelot,Y. (2006) Colon–pecific drug delivery:Influence of Solution reticulation properties upon pectin beads performance. International Journal of Pharmaceutics, 321, 86-93.

Chignell, C.F., Bilski, P., Reszka, K.J., Motten, A.G., Sik, R.K. and Dahl, T.A. (1944) Spectral and photochemical properties of curcumin. Photochemistry and Photobiology, 59, 295-302.

Cho, H.G. and Andrews, L. (2011) Infrared spectra of CH_3-MF and several fragments prepared by methyl fluoride reactions with laser-ablated Cu, Ag, and Au atoms. Inorganic Chemistry, 50, 10319-10327.

Dai, J., Wu, S., Jiang, W., Li, P., Chen, X., Liu, L., Liu, J., Sun. D., Chen, E., Chen, B. and Shengli, F. (2013) Facile synthesis of Pectin coated Fe_3O_4 nanospheres by the sonochemical method. Journal of Magnetism and Magnetic Materials, 331, 62-66.

DeRosa, M.C. and Crutchley, R.J. (2002), Photosensitized singlet oxygen and its applications. Coordination Chemistry Reviews, 233-234, 351-371.

Hu, Y., Kanka, J., Liu, K., Yang, Y., Wang, H. and Du, H. (2016) Gold nanoring - enhanced generation of singlet: an intricate correlation with surface plasmon resonance and polyelectrolyte bilayers. RSC Advances, 7, 104819-104826.

Huang, P., Xu, C., Lin, J., Wang, C., Wang, X., Zhang, C., Zhou, X., Shouwu, G. and Cui, D. (2011) Folic acid conjugated graphene oxide loaded with photosensitizers for targeting photodynamic therapy. Theranostics, 1, 240-250.

Iijima, M., Nakamura, K., Hatakeyama, T. and Hatakeyama, H. (2000) Phase transition of pectin with sorbed water. Carbohytrate polymers, 41, 101-106.

Jiang, G., Wang, L. and Chen, W. (2007) Studies on the preparation and characterization of gold nanoparticles protected by dendrons. Materials Letters, 61, 278-283.

Levy, H.B., Gennady, E., Shter, G.E., Grader, G.S. and Avnir, D. (2004) Entrapment of organic molecules within metals-polymers in silver. Chemistry of Materials, 16, 3197-3202.

Manju, S. and Sreenivasan, K. (2012) Gold nanoparticles generated and stabilized by water soluble Curcumin- polymer conjugate: Blood compatibility evaluation and targeted drug delivery on to cancer cells. Journal of Colloid and Interface Science, 368, 144-151.

Manson, J., Kumar, D., Meenan, B.D. and Dixon, D. (2011) Polyethylene glycol functionalized gold nanoparticles: the influence of capping density on stability in various media. Journal of Gold Bulletin, 44, 99-105.

Michael, F.C., Fryer, J., Reeder, B., Bechtold, U., Mullineaux, P.M., Nonell, S., Wilson, M.T. and Brake, N.R. (2006) Imaging the production of singlet oxygen invivo using a new fluorescent sensor, singlet oxygen sensor Green. Journal of Experimental Botany, 57, 1725-1734.

Oh, J., Yoon, H. and Park, J.H. (2013) Nanoparticle platforms for combined photothermal and photodynamic therapy. Biomedical Engineering Letters, 3, 67-73.

Ouajai, S. and Shanks, R.A (2005) Composition, structure and thermal degradation of hemp cellulose after chemical treatments. Polymer Degradation and Stability, 89, 327-335.

Park, G., Seo, D., Chung, L.S. and Song, H. (2013a) PEG and carboxylate- functionalized nanoparticles using polymer linkeges: Single-step synthesis, high stability, and plasmonic detection of proteins. Langmuir, 29, 13518-13526.

Park, H.H., Park, S.J., Ko, G. and Woo, K. (2013b) Magnetic hybrid colloids decorated with Ag nanoparticles bite away bacteria and chemisorb viruses. Journal Materials Chemistry B, 1, 2701-2709.

Schmidbaur, H., Raubenheimer, H.G and Dobrzanska, L. (2013) The gold-hydrogen bond, Au-H, and the hydrogen bond to gold, Au···H-X. Chemical Society Reviews, 43, 345-380.

Sutar, P.B., Mishra, K., Pal, K. and Banthiya, A.K. (2008) Development of pH sensitive polyacrylamide grafted pectin hydrogel for controlled drug delivery system. Journal of Materials Science: Materials in Medicine, 19, 2247-2253.

Wang, F., Chen, X., Zhao, Z., Tang, S., Huang, X., Lin, C., Caib, C., and Zheng, N. (2011) Synthesis of magnetic, fluorescent and mesoporous core-shell-structured nanoparticles for imaging, targeting and photodynamic therapy. Journal of Materials Chemistry, 21, 11244-11252.

Zeitouni, N.C., Oseroff, A.R. and Shieh, S. (2003) Photodynamic therapy for nonmelanoma skin cancers current review and update. Molecular Immunology, 39, 1133-1136.

Zhang, Y., Aslan, K., Previte, M.J.R. and Geddes, C.D. (2007) Metal-enhanced singlet oxygen generation: a consequence of plasmon enhanced triplet yields. Journal of Fluorescence, 7, 345-349.

Zhao, L., Kim, T.H., Ahn, J.C., Kim, H.W and Kim, S.Y. (2013) Highly efficient theranostics system based on surface-modified gold nanocarrires for imaging and photodynamic therapy of cancer. Journal of Materials Chemistry B, 1, 5806-5817.